Viking Mars Hydrazine Terminal Descent Engine Thermal Design Considerations

Charles R. Cunningham* and Donald C. Morrisey†
Rocket Research Corporation, Redmond, Wash.

A description is given of some of the more significant thermal design considerations employed in the development and qualification of the monopropellant hydrazine terminal descent engines on the Viking Mars lander spacecraft. The terminal descent engine operates in a blowdown and throttling mode, which results in an operating thrust range of 638 to 90 lbf. Martian entry thermal design boundary conditions are described, along with resulting radiative and conductive engine thermal isolation hardware. Test results are presented, showing engine thermal design performance as compared with specified requirements. General engine materials of construction are described, along with Hastelloy B shell structural characteristics, which were extended to 2000°F by test and are compared with limited existing MIL-HDBK-5 data. Subscale test results are presented, showing the maximum catalyst bed cylinder design temperature of 1970°F. Test results also are presented, showing local reactor internal convective heat-transfer coefficients. Such data are unique, since the engine employs a completely radial flow catalyst bed design. This design approach is the first of its kind in the monopropellant hydrazine gas generator field to be flight qualified.

Nomenclature

LCH = low cost hydrazine catalyst
MA = maximum allowable
MC = maximum calculated
MLI = multilayer superinsulation
RCS = reaction control system 5.0-lbf thrusters
REA = rocket engine assembly
T = temperature, °F
T_G = hydrazine decomposition flame temperature, °F
VLC = Viking lander capsule
$\dot{w}$ = propellant flowrate, lbm/sec
X = fractional ammonia dissociation
ΔH = hydrazine heat of decomposition, Btu/lbm
ϵ = emittance
σult = ultimate stress, ksi
σ_{yp} = yield stress, ksi

Introduction

THIS article discusses thermal characteristics of the Viking Mars lander spacecraft terminal descent braking engines, designed to effect a soft landing on the planet Mars. The engines only fire for 45 sec during descent to the planet surface; however, there is a relatively longer, 35-hr, and 10-min transient orbit and deorbit period prior to entering the Martian atmosphere which requires extensive active and passive engine thermal control.

Thermal control of the engine catalyst bed and propellant valve had to be examined carefully via extensive analysis and test verification in order to keep from unfavorably impacting the limited spacecraft electrical power supply and the delicate spacecraft/engine interface transient heat balance. The analysis dictated, and the testing verified, an array of radiative and conductive thermal isolation hardware, which in essence optimized the engine nonfiring time constant for the 5-hr, 10-min deorbit period.

Received June 25, 1976; revision received Sept. 3, 1976.
Index categories: Thermal Modeling and Experimental Thermal Simulation; Spacecraft Propulsion Systems Integration; Liquid Rocket Engines.

*Thermal Engineering Specialist and Overall Viking RCS and Terminal Descent Engines Responsible Thermal Engineer. Member AIAA.
†Vice-President Aerospace Products Division and Overall Viking RCS and Terminal Descent Engines Program Manager. Member AIAA.

The previously mentioned array of radiative and conductive thermal isolation hardware will be described subsequently. Three engines are employed per spacecraft. The most unique feature of these engines is their completely radial flow catalyst bed design. The engine is shown in Fig. 1. This REA represents the first flight-qualified use of a completely radial flow catalyst bed design in the monopropellant hydrazine gas generator field. More recent advanced versions of the Viking engine design have been developed and qualified, and one relatively long-life version is reported in Ref. 1.

This article contributes some interesting thermal design characteristics of such hydrazine engines employing radial flow catalyst bed designs. In addition, it indicates the precision and accuracy of current sophisticated analytical heat-transfer technology being employed in the aerospace industry, and especially in radiation analysis. Thermal boundary conditions used for analysis of components on a spacecraft that orbits, enters the atmosphere of, and lands on the planet Mars are presented. Corresponding simulation testing is discussed, along with analytical and test result thermal model correlations.

Some basic thermal/structural analyses and test results are presented. Such data were utilized to predict maximum local temperatures and select corresponding allowable stresses for structural design. Data from MIL-HDBK-5 for Hastelloy B, the basic engine material, was available only to 1600°F. Specific structural testing was performed during engine development to extend such knowledge to 2000°F. Corresponding structural allowable data are presented.

Thermal Design Description

Material and part arrangement details are depicted in Fig. 2, with part or nodal definitions listed in Table 1. Nodes 2, 3, and 28 represent the basic spacecraft interface hardware. Propellant tanks (node 3) within the spacecraft supply pressurized fuel up to a pyrovalve (node 28), which is attached to the spacecraft. The pyrovalve is radiatively isolated with MLI and conductively isolated with high resistance standoffs. The REA is attached to an aluminum spacecraft bracket.

The basic pressure vessel, including nozzles, injector, and catalyst bed cylinders, is constructed of high-temperature heat resistant Hastelloy B. Not clearly shown are the 18 nozzles, 6 in an inner ring (nodes 25 and 37) and 12 in an outer ring configuration (nodes 24 and 36). The multinozzle design was

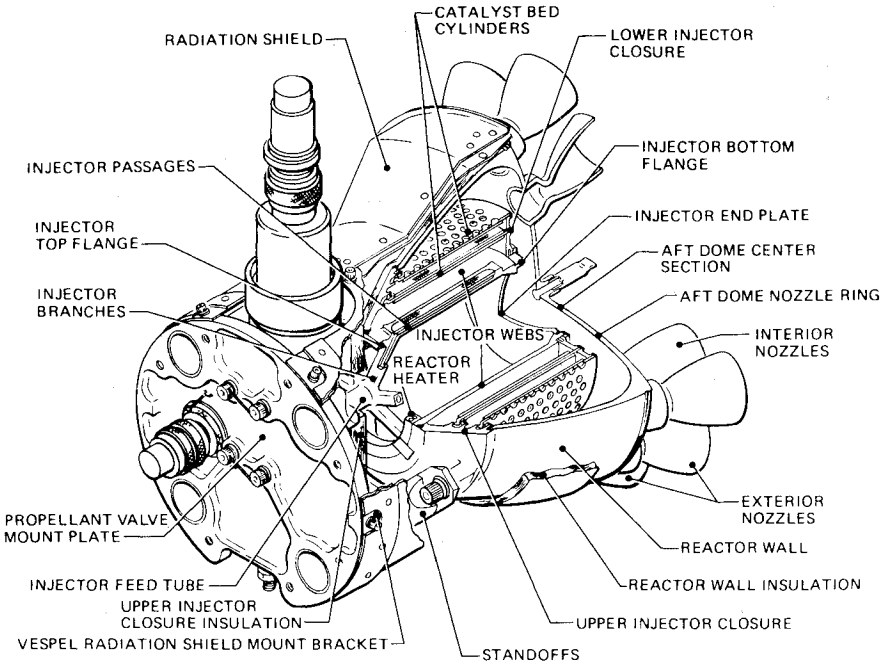

Fig. 1 Viking Mars lander spacecraft terminal descent monopropellant hydrazine engine.

chosen in order to minimize plume disturbance of the Martian surface upon landing. The propellant valves consist of an isolation pyrovalve (node 28) and an axial displacement torque motor driven throttle valve (nodes 4, 5, and 35).

Propellant contained upstream of the pyrovalve is maintained above freezing by the spacecraft thermal control system; while downstream in the dry REA throttle valve, metal temperatures are allowed to fall below the propellant freeze range, 35°-37°F. Upon pyrovalve actuation just prior to engine firing, a surge flow of propellant traverses the partially opened throttle valve and flows into the engine.

Extensive testing verified that throttle valve flow passage temperatures as low as −15°F could be tolerated with the initial minimum 10% opening in the metering section before any flow blockage due to freezing would occur. The propellant enters the throttle valve at a minimum of 45°F and the simultaneous heat exchange immediately brings all relatively lower thermal capacity metal flow passages above freezing.

This dynamic energy exchange method of heating the REA throttle valve was utilized to conserve spacecraft power allocated for REA preheating prior to operation. Thus, any need for active heating of the REA throttle valve was eliminated. All valve materials of construction are primarily stainless steel 304L because of its recognized compatibility with hydrazine.

A redundant element heater is provided to warm the catalyst bed directly to insure smooth engine starting. Indirectly, this heater (node 30) also provides warming of the throttle valve to prevent flow blockage due to hydrazine freezing. As previously mentioned, tests showed that the throttle valve at the pintle housing (between nodes 4 and 5) has to be at or above −15°F prior to start to prevent flow blockage caused by freezing. Experimental testing demonstrated successful engine starts at bed temperatures as low as 17°F; and 45°F was selected as a nominal design point to provide margin and assure repeatable smooth start transients. Such tests were performed to simulate a heater element half-power failure mode. At full power, all tests showed that the heater maintains catalyst bed and throttle valve well above minimum temperature limits mentioned previously.

In operation, the heater actively warms operational engine components well above minimum throttle valve and previously mentioned catalyst bed temperature limits. While lander and parent orbiter spacecraft are still joined in orbit

Table 1 Nodal descriptions

1.	Capsule int or Mars surface[a]	23.	Reactor wall insulation
2.	Lander attach structure[a]	24.	Exterior nozzle bells
3.	Propellant in capsule[a]	25.	Interior nozzle bells
4.	TV filter housing	26.	Mars atmosphere recovery temperature
5.	TV actuator housing	27.	Lower radiation shield
6.	Mount plate	28.	Pyro valve
7.	Standoffs	29.	Upper radiation shield
8.	⑦⑧ interface	30.	Reactor heater
9.	Upper injector closure	31.	Heat soakback rate
10.	⑦⑨ interface	32.	Accumulative soakback
11.	Closure insulation	33.	Injector webs
12.	Injector branch tubes	34.	Propellant flow rate
13.	Injector passages	35.	TV armature
14.	Top injector flange	36.	External nozzle throat
15.	Propellant feed tube	37.	Internal nozzle throat
16.	Bottom injector flange	38.	Feed tube N_2H_4 discharge
17.	Injector end plate	39.	Branch N_2H_4 discharge
18.	Lower injector closure	40.	Passage N_2H_4 discharge
19.	Catalyst bed/hot gas	41.	REA total weight
20.	Aft dome center section	42.	Heater leadwire center
21.	Aft dome nozzle ring	43.	Heater leadwire insulation
22.	Reactor wall	44.	Electrical connector

[a]Boundary conditions.

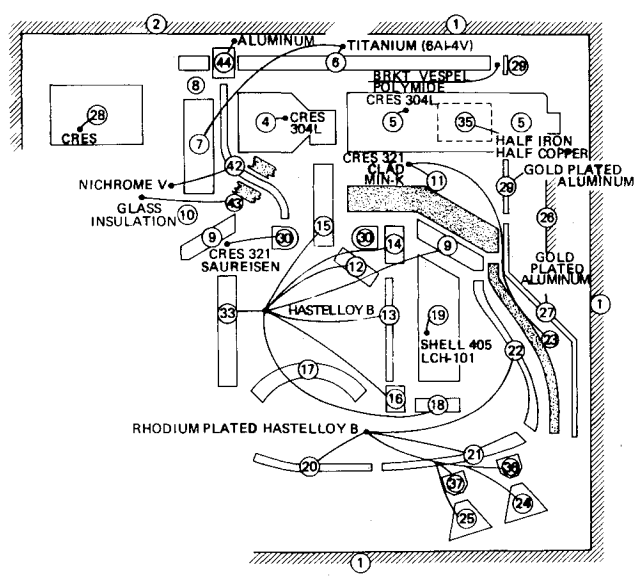

Fig. 2 VLC-REA materials description.

around Mars, the descent engine heaters are turned on for 30 hr. At the end of this period, heater power is shut off with the catalyst bed nominally at 139°F and the throttle valve pintle houseing at 10°F when the lander spacecraft separates from its parent orbiter vehicle and starts a 5-hr, 10-min descent to the edge of the Martian atmosphere.

During the 5-hr, 10-min deorbit period with no heater power, the engine thermal isolation system passively keeps critical engine components such as throttle valve and catalyst bed from falling below their respective limit values of −15° and 17°F. The engine thermal isolation system resulting from extensive thermal analysis consists of four basic components, shown in Fig. 2.

First, relatively high strength and low thermal conductiveity titanium standoffs, 6A1-4V, structurally isolate the reactor and catalyst bed sections of the engines from the spacecraft mounting interface. Four standoffs are used, which result in a total conductive resistance of 17.0 hr-°F/Btu. Second, added thermal isolation is provided by a fibrous insulation blanket of low thermal conductivity wrapped around the reactor. The insulation blanket covering the bell section of the reactor (node 23) is ⅛ in. thick, and the blanket covering the top injector closure section of the reactor (node 11) is ½ in. thick.

The insulation blanket is foil clad with unpolished, crinkled, and control vented 2-mil 321 stainless steel. Filters are placed in each vent to assure that the hot engines do not permit insulation material to escape during landing. The size of the filters was 25 μ. The actual insulation material chosen was the fibrous "high-temperature flexible Min-K," of density 16 PCF, thermal conductivity 0.01 Btu/hr-ft-°F, covered with quartz cloth, and all stitched in a pattern of small squares with lubricated quartz thread. A baking of the final blanket assembly at 500°F for 30 min was employed to insure that the lubricant was eliminated prior to use on the engine.

Third, radiation heat loss from the engine aft dome (nodes 20 and 21) and nozzles (nodes 24, 25, 36, and 37) is reduced by plating these surfaces with low-emittance rhodium. Rhodium was required instead of gold for high-temperature applications (greater than 800° to 1200°F). Plating substrate surface finish goals in the neighborhood of 32 μin. rms were required to insure an emittance ranging from 0.05 to 0.09. Aft dome and nozzles are plated inside and out, but no specific surface finish requirements were designated for the inside of the aft dome. There, an emittance of 0.25 was assumed for analysis.

Fourth, radiation heat loss from all other exposed surfaces of the engines outside of the aft dome and nozzles is reduced with a gold-plated thin aluminum radiation shield. The plating was applied to both sides of the shield after obtaining a surface finish of 16 μin. rms, which insured an emittance ranging from 0.03 to 0.05. The effectiveness of the radiation shield was guaranteed by providing sufficient attachment conductive resistances as optimized by analysis.

The shield is supported by a bracket from engine standoff mount plate (node 6) and spring tabs at the intersection of the aft dome (node 21) and the reactor wall (node 22). The spring tabs are stainless steel, and actually touch the Min-K insulation blanket, not the reactor metal. The total tab conductive resistance is 26.6 hr-°F/Btu. The main support bracket was machined from DuPont Vespel polyimide plastic to obtain a conductive resistance of 50.0 hr-°F/Btu. A thermal conductivity of 0.20 Btu/hr-ft-°F was used for Vespel.

Thermal Design Requirement Conformance

The engine thermal design features mentioned in the previous section were dictated by the following specified requirements. These thermal design goals are listed as follows, in a descending order of thermal complexity:

1) Maintain the minimum catalyst bed temperature greater than 45°F prior to engine ignition in order to insure a smooth engine start. In accomplishing this requirement, no more than a 9.8-W heater power drain per engine is allowed in order to conserve spacecraft power. The 9.8 W correspond to the minimum expected spacecraft voltage supply tolerance and the maximum expected REA heater element resistance tolerance.

2) Never allow external surface temperatures to exceed 875°F in order to limit radiation heat transfer to the spacecraft. This does not apply to the nozzles and aft dome sections of the engines, for they are located below the spacecraft in a position of insignificant geometric radiative view.

3) Keep conduction heat transfer during the first hour after landing on the Martian surface below 90 Btu in order to limit heat transfer to the lander support structure.

4) Maintain the throttle valve pintle housing above −15°F to insure against propellant freezing and to guarantee engine starting in a cold environment under dynamic conditions with initial 45°F propellant surge flow through the partially opened and initially dry REA throttle valve.

5) Maintain pyrovalve heat leak to the throttle valve below 1.0 W in order to insure pyrovalve heater adequacy.

Absolute conformance with the previously specified thruster design requirements, based on extensive test and analyses, was achieved and demonstrated as summarized in Fig. 3, on which test results substantiating the analytical predictions are listed. Figure 4 gives heater performance vs catalyst bed temperature. Both test and analysis data result from 35-hr, 10-min transient simulation of orbit and deorbit periods prior to Martian atmospheric entry. As shown, the specification requirement to maintain the catalyst bed above 45°F is met with minimum heater power of 9.8 W. Furthermore, if one heater coil fails, the corresponding minimum power available is 4.9 W and Fig. 4 shows that a satisfactory catalyst bed temperature of 17°F can be maintained.

As shown in Figs. 3 and 4, the experimental results of the thermal vacuum tests on the development engine substantiate

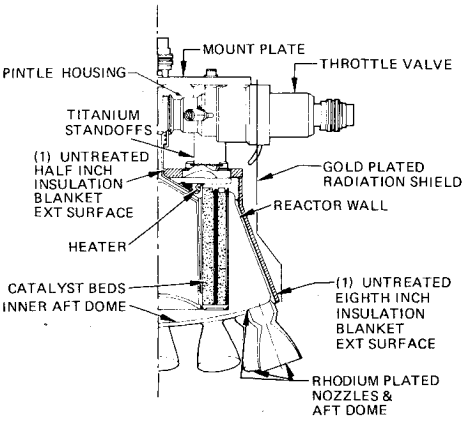

(1) MIN-K, "HIGH TEMPERATURE FLEXIBLE", 16 PCF

- CATALYST BED TEMPERATURE AT IGNITION ... 52°F (52°F)*
  - ASSUMES COLD ENVIRONMENT
  - SPECIFICATION ..... >45°F
- THROTTLE VALVE PINTLE HOUSING AT IGNITION ..... -2°F (-5°F)
  - ASSUMES COLD ENVIRONMENT
  - DESIGN GOAL ..... >-15°F
- REA MAXIMUM SURFACE TEMPERATURE ..... 748°F (660°F)
  - ASSUMES HOT ENVIRONMENT
  - EXCLUDES NOZZLES & AFT DOME
  - SPECIFICATION ..... <875°F
- MAXIMUM PYRO VALVE HEAT LEAK ... 0.9 WATT (0.7 WATT)
  - ASSUMES COLD ENVIRONMENT
  - SPECIFICATION ..... <1.0 WATT
- REA MAXIMUM HEAT SOAKBACK TO LANDER STRUCTURE
  - HOT ENVIRONMENT ..... 65 Btu (62 Btu)
  - COLD ENVIRONMENT ..... 68 Btu (83 Btu)
  - SPECIFICATION ..... <90 Btu

*EXPERIMENTAL RESULTS IN PARENTHESIS

Fig. 3 Summary of flight configuration thermal performance vs specification requirements.

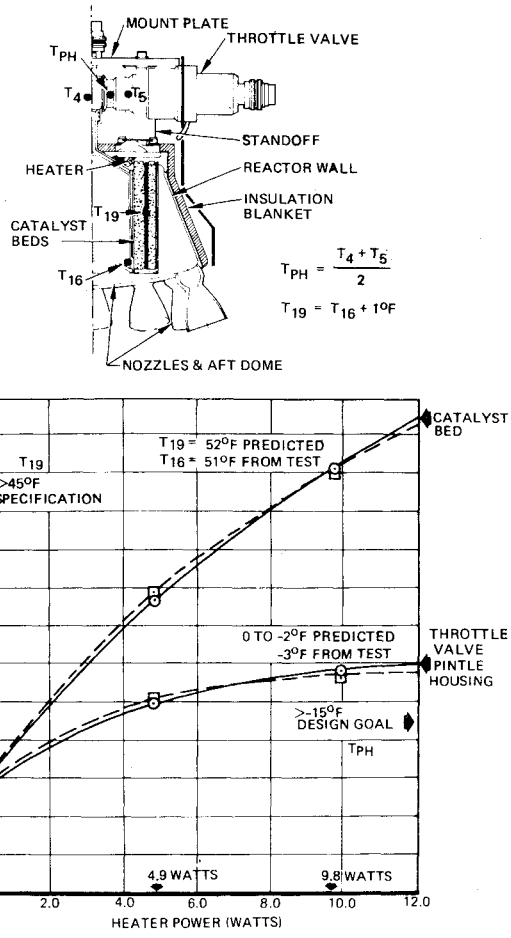

Fig. 4 Heater power vs catalyst bed temperature for a cold environment.

the calculated results to an acceptable degree. All thermal vacuum testing was accomplished in diffusion pump equipped chambers at pressures ranging from 0.0001 to 0.00007 Torr. Note in Figs. 3 and 4 that the minimum catalyst bed temperature predicted by the thermal analysis with 9.8 W is 52°F, which is in full agreement with test. These results depict the precision and accuracy of current state-of-the-art thermal analytical technology and methods, which will be described subsequently.

The minimum catalyst bed temperature obtained during the testing with 4.9 W agrees with the analytical predictions to within 2°F. The predicted value is on the conservative side. The minimum throttle valve pintle housing temperature data, with both 9.8 and 4.9 W of applied power, agree within 3°F, and are safely above the −15°F desired limit established by component flow blockage tests.

The pyrovalve heat leak analytical prediction is within 0.2 W of the measured value, and on the conservative side. The experimental pyrovalve heat leak of 0.7 W was calculated using the experimental temperature differences and an estimated minimum value of conductive resistance.

As shown in Fig. 3, the second and third thermal design requirements were substantiated with adequate margins. The REA maximum surface temperature was predicted to be 748°F, whereas test temperatures never exceeded 660°F. With respect to this difference, it is of interest to mention that a Min-K thermal conductivity of 0.03 Btu/ft-hr°F is used for hot firing analyses, providing a conservative maximum prediction of the surface temperature.

Finally, the test temperature distributions substantiated that the 90-Btu maximum allowable soakback from the REA to the spacecraft, after engine firing is terminated, also was satisfied.

Thermal Analysis Boundary Conditions

The thermal design features of the REA and the analytical results previously were based on time periods of 30-hr heater power on prior to Martian atmospheric entry, termed "Mars orbit"; 5-hr, 10-min heater power off after separation of lander, termed "deorbit"; 644 sec of atmospheric flight, termed "atmospheric entry and aerodeceleration"; 45 sec of engine firing to affect the soft landing, termed "terminal descent and landing"; and a 1-hr heat soakback period after landing, during which time a maximum of 90 Btu can be conducted to the spacecraft through the engine mount brackets.

Particular spacecraft flight configurations, corresponding with previously mentioned time periods, are depicted in Fig. 5. Environmental engine radiation/conduction/convection boundary conditions are listed in Tables 2 and 3. Such boundary conditions are characterized as heat sources and heat

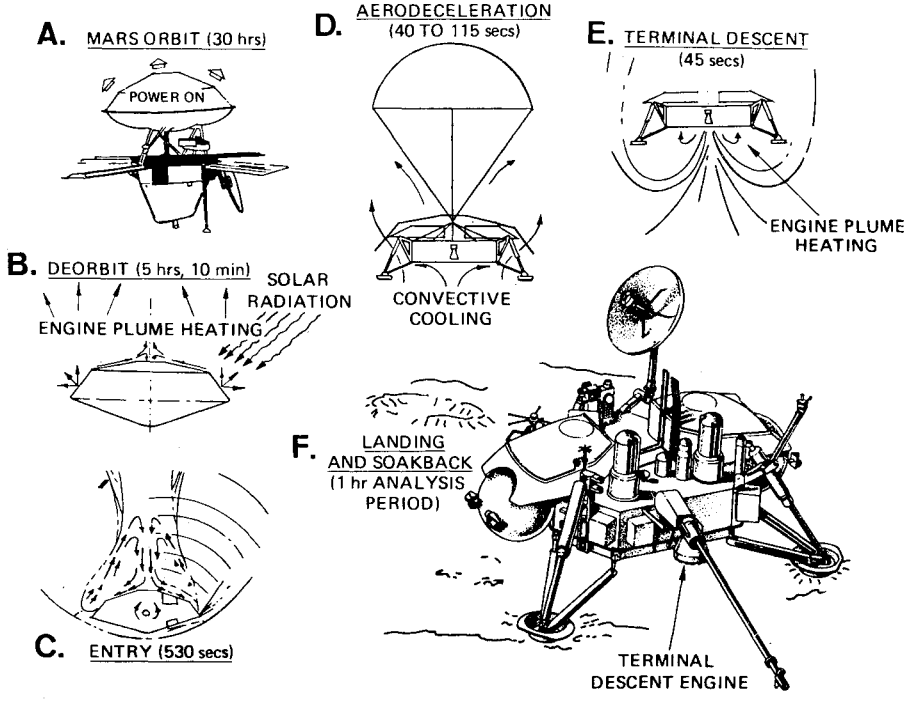

Fig. 5 Primary events at Mars affecting REA thermal design.

Table 2 Detailed breakdown of VLC-REA duty cycle (Mars orbit and entry deorbit phase)

	Thermal Environment Characteristics		
Phases	Duration	Heat Source Characteristics	Heat Sink Characteristics

• Mars orbit	• 30 hrs	• Catalyst bed heater powers
		  • 12.5 watts for hot environment
		  • 9.8 watts for cold environment
		• Pyro valve – Varies from -35°F linearly to +45°F
			• Radiation – Black body enclosure at -35°F (cold) and +125°F (hot)
			• Conduction – Infinite capacity attachment at -35°F (cold) and +125°F (hot)

• Deorbit	• 5 hrs 10 mins	• Pyro valve – Remains at +45°F at throttle valve filter section interface	• Radiation – Black body enclosure at -35°F (cold) and +125°F (hot) • Conduction – Infinite capacity attachment varying same as above
• Atmospheric entry	• 530 secs	• Maximum heating – The black body enclosure varies linearly from +125 to 300°F at 3.5°F/sec, and remains at 300°F for the duration (hot)	• Minimum Heating – The black body enclosure is maintained at deorbit conditions (cold)
• Aerodeceleration	• 115 secs (cold) • 40 secs (hot)	• None	• Radiation – Black body enclosure at -35°F (cold) and +125°F (hot) • Conduction – Infinite capacity attachment at -35°F (cold) and +125°F (hot) • Convection – Recovery temperatures, -150°F (cold), +25°F (hot), and aeroheating coefficients 0.8 Btu/ft^2-hr-°F (cold) and 1.2 Btu/ft^2-hr-°F (hot)

Table 3 Detailed breakdown of VLC-REA duty cycle (terminal descent and landing phases)

	Thermal Environment Constraints		
Phases	Duration	Heat Source Characteristics	Heat Sink Characteristics
• Terminal descent and landing	• 45 secs	• Catalytic decomposition of hydrazine according to the following procedure: • Calculate percent NH_3 dissociation emperically from: $X = 0.54 - 0.0775(\dot{w} - 2.7)$ • Propellant flow rate, .7 to 3 lbm/sec initially, 2.2 lbm/sec near end firing according to the worst-case blowdown schedule • Calculate heat of decomposition and flame temperature semi-empirically from: $\Delta H = 1{,}503 - 825X$ $T_G = 2{,}525 - 1{,}422X$	• Radiation – Black body Martian surface at -35°F (cold) and +125°F (hot) • Conduction – Infinite capacity attachment at -35°F (cold and +125°F (hot) • Convection – Recovery temperatures -150°F (cold) and +265°F (hot), and aeroheating coefficient 1.4 Btu/ft^2-hr-°F (hot or cold)
• Soakback (after landing)	• 1 hour	• Heat stored in REA after 45-sec firing	• Radiation – Black body Martian surface at -35°F (cold) and +125°F (hot) • Conduction – Infinite capacity attachment, -35°F (cold) and +125°F (hot) • Convection – Martian atmosphere, -35°F (cold), +125°F (hot) with free convection coefficient, 0.1 Btu/ft^2-hr-°F

sinks. Reactor ammonia dissociation relations (which affect gas temperature) were determined empirically for the 45-sec terminal descent and landing phase. All other environmental conditions, listed in Tables 2 and 3, were specified as the basis for engine thermal analysis and design. Cold boundary conditions are assumed in the analysis when predicting the adequacy of the thermal design to keep the catalyst bed and throttle valve above respective 17° and −15°F limits discussed previously. Hot boundary conditions are assumed in the analysis when predicting the adequacy of the thermal design to prevent component overheat, and to predict maximum part local temperatures for structural design.

Thruster Thermal Analysis Technology

In general, nodal finite-difference heat-balance equations are solved on a CDC 6600 computer with the general application, multinodal capacity, thermal analyzer program of Ref. 2. Transient solution of the network heat balance equations employs an exponential explicit formulation of the nodal differential equations. Equilibrium or steady-state solution of the network heat balance equations employs a rapidly converging relaxation scheme.

The program calculates radiant interchange factors for multisurface enclosures based upon the classical Oppenheim network method of Ref. 3. Thus, all surfaces are assumed diffuse and gray. Standard matrix technique employed for solution. The previously described thermal analyzer program is mathematically similar to other thermal analyzer programs such as those of Refs. 4 and 5, which are industry standards.

The thermal analyzer program of Ref. 2 has network multiplication and subprogramming capability, which allows special hydrazine reactor routines to be added for calculating multi-engine installation effects and injector fluid flow temperature change, including freezing, boiling, and decomposition effects. Furthermore, special subroutines are available for calculating effects of temperature on ammonia dissociation, thermal conductivity, and specific heat.

In particular, for the terminal descent engine thermal analysis, a thermal model was programmed into the thermal analyzer which included 37 basic nodes, 27 convection resistances, 51 conduction resistances, and 55 radiant interchange factors. The radiation analysis was the most significant and the engine was modeled as six separate enclosures. The resulting radiation network is shown in Fig. 6. Nodal definitions have been given previously in Table 1.

Significant Nonfiring Results

The most significant thermal test results already have been given in Fig. 3, where conformance is shown by test and analysis with all of the specified thermal design requirements. As shown in Fig. 3, the analysis predicted that the catalyst bed would be 52°F after the 35-hr, 10-min orbit and deorbit

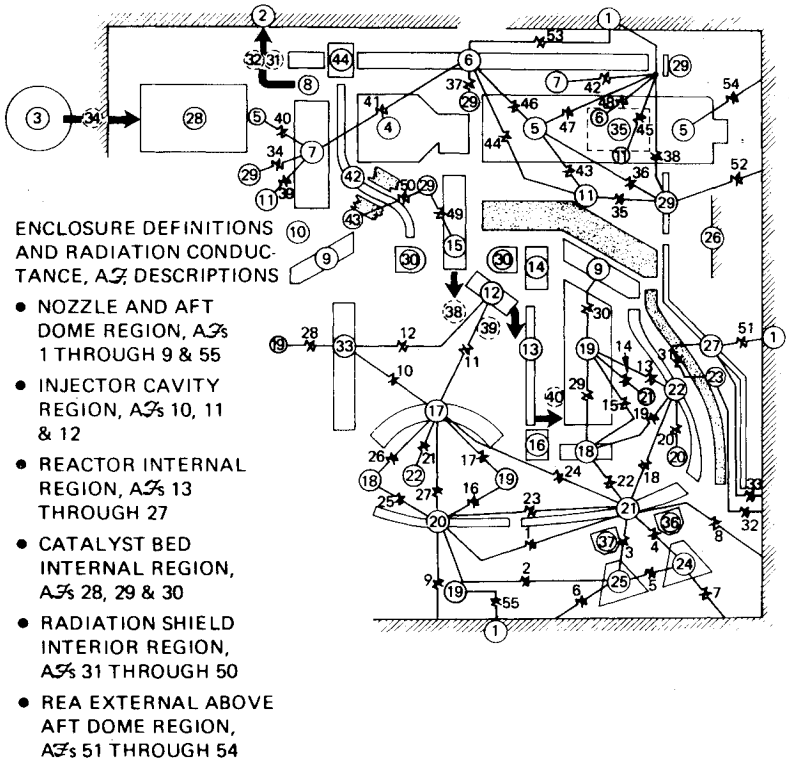

Fig. 6 VLC-REA radiation thermal network.

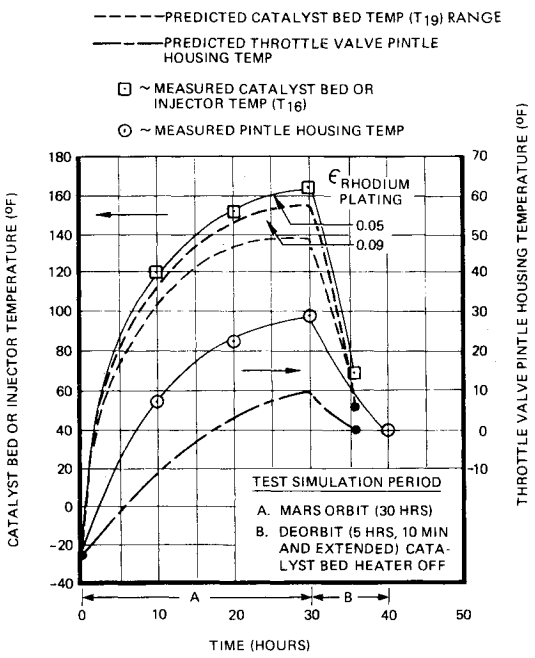

Fig. 7 Thermal vacuum qualification test results.

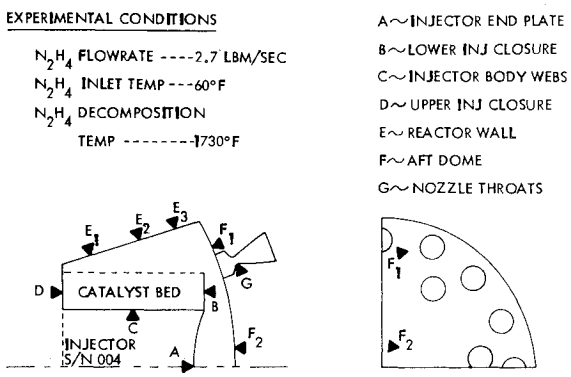

LOCATION	VALUE	LOCATION	VALUE
A	75	E_2	295
B	365	E_3	180
C	430	F_1	160
D	365	F_2	75
E_1	365 to *215	G	200

*LOWER VALUE REPRESENTS A LOCAL CIRCUMFERENTIAL VARIATION DUE TO LOCAL HIGH BED LOADING EFFECTS

Fig. 8 Viking lander REA internal convective heat-transfer coefficients.

periods. Futhermore, the 35-hr, 10-min thermal vacuum test verified the 52°F exactly. A subsequent thermal vacuum test was performed during qualification, and the results are presented in Fig. 7. As shown, the catalyst bed minimum temperature was 68°F.

The predicted number of 52°F was based upon worst-case analysis, utilizing the maximum expected rhodium plated surface emittance of 0.09 for conservatism. For the Viking REA, any change in the value of emittance of the rhodium plated aft dome and nozzle surfaces was of primary significance in affecting minimum catalyst bed temperature. The thermal model radiation network of Fig. 6 showed that the change in catalyst bed temperature was equal to 4°F for every 0.01 unit change in rhodium plating emittance. Therefore, if the emittance value is improved from 0.09 to the minimum expected value of 0.05, the predicted catalyst bed temperature increases from 52° to 68°F. Post-test emittance checks tended to verify that the test articles varied from each other in this regard.

It should be mentioned that the test results from Figs. 3 and 7 were obtained from two separate engines. The results from Fig. 3 are based on a developmental engine, and such engines usually have suffered more degradation than engines submitted for qualification testing. The logic behind this approach is to insure that the qualification test results will come out better, as is the case in Fig. 7.

As previously mentioned, a design limit of −15°F was established during the development test program for the throttle valve pintle housing, which locally is assumed to be the average of actuator and filter housing temperatures. As

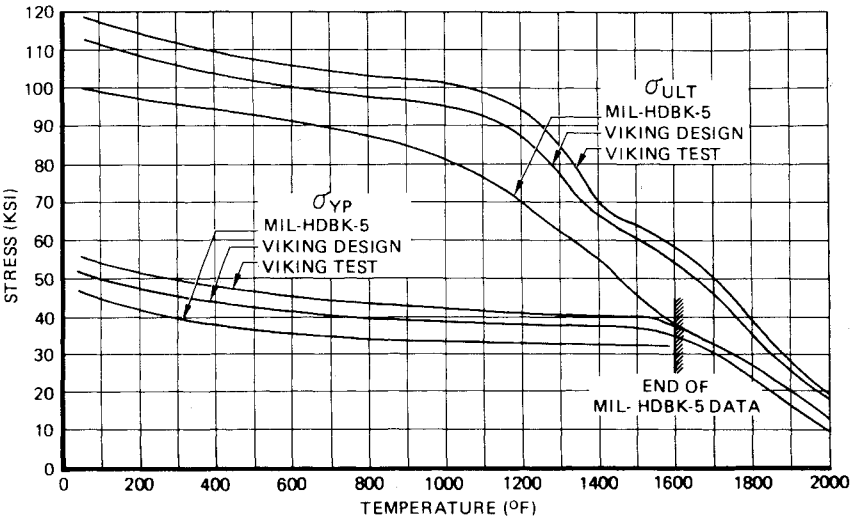

Fig. 9 Hastelloy B structoral allowables beyond MIL-HDBK-5 data.

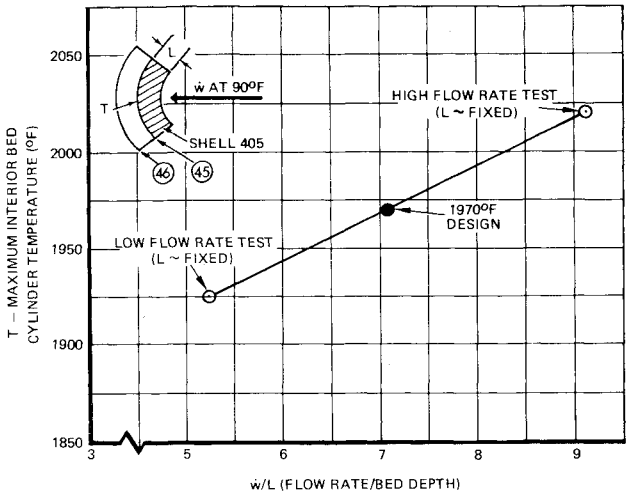

Fig. 10 Subscale VLC-REA catalyst bed cylinder design temperatures.

also verified by the thermal vacuum test results presented in Fig. 7, this temperature was met even at the end of a cold environment soak period lasting 4 hr, 50 min past the 5-hr,10-min deorbit period.

Significant Hot Firing Results

During firings, in order to predict nodal or engine part temperatures accurately for structural design, the internal convective heat-transfer coefficients first must be known. A strictly empirical approach was taken utilizing local wall thermocouple measurements, an average gas stream temperature measurement, and a knowledge of local wall thickness at corresponding thermocouple locations. This basic method is not new, but a good explanation appears in Ref. 6.

Resulting maximum local convective heat-transfer coefficients are given in Fig. 8. Using such values, excellent correlations of the thermal model with local wall temperature measurements appear in Ref. 6. Thus, a high confidence level can be placed in the heat-transfer coefficients listed in Fig. 8.

Maximum engine part temperatures were calculated for structural design and are given in Table. 4. Since nearly all Hastelloy B pressure vessel shell and nozzle temperatures are above the 1600°F limits of MIL-HDBK-5, high-temperature structural testing was performed on typical Hastelloy B samples from reactor material stock. The results of the tests, giving high-temperature structural allowables, are shown in Fig. 9. More details of the data shown in Fig. 9 are documented in Ref. 7.

Table 4 Comparison of maximum allowable part temperatures with predictions

Node No.	Part Name	T_{MA} (°F)	T_{MC} (°F)
4, 5, 35	Propellant valve	300	271
6	Mount plate	1,000	265
7	Standoffs	1,000	634
9	Upper injector closure	1,540	1,540
11	Upper injector closure insulation	1,800	1,700
12	Injector branches	1,800	1,540
13	Injector passages	1,800	1,560
14	Injector top flange	1,450	1,400
15	Injector feed tube	1,000	757
16	Injector bottom flange	1,775	1,760
17	Injector end plate	1,775	1,760
18	Lower injector closure	1,900	1,900
20	Aft dome center section	1,800	1,650
21	Aft dome nozzle ring	1,770	1,730
22	Reactor wall	1,965	1,950
23	Reactor wall insulation	1,800	1,770
24, 36	Exterior nozzles	1,800	1,650
25, 37	Interior nozzle	1,800	1,650
27, 29	Radiation shield	900	748
30	Reactor heater	1,600	1,440
33	Injector webs	1,850	1,830
43	Heater leadwire insulation	1,000	638
----	Vespel radiation shield mount bracket	800	638
45, 46	Catalyst bed cylinders	1,970	1,970

Interior catalyst bed cylinder maximum design temperatures were obtained from subscale test results as shown in Fig. 10. A 1/12 segment of the catalyst bed was instrumented with interior bed thermocouples located on the inner bed plate. The flowrate was varied and the resulting bed cylinder temperature variation is shown in Fig. 10. The 1970°F value corresponds to a peak Viking flowrate of 2.96 lbm/sec and a bed cylinder dimension of 0.415 in.

Conclusions

Thermal vacuum test results on the Viking lander descent engine have shown excellent correlation with predicted results, as those in Figs. 4 and 7. The resulting correlation reaffirms the accuracy of current state-of-the-art sophisticated analytical heat-transfer technology. The engine temperature distributions are markedly affected by radiation, and test results demonstrate that the Oppenheim network method of Ref. 3, used to obtain the network components of Fig. 6, provides very accurate results.

Employment of this classical method is inherently based upon the assumptions of diffuse and gray surfaces; and more sophisticated specular-diffuse and nongray methods of analysis are available to extend the diffuse and gray limitation. However, results presented herein, as those in Fig. 4, demonstrate that the assumptions of diffuse and gray surfaces do not represent any significant analytical limitations.

In fact, the author of Ref. 8 states that he has omitted any radiation analysis techniques based on specularly reflecting surfaces from his book because, from his research, analyses based on diffuse models are in excellent agreement with experiment for industrial surfaces.

Acknowledgment

Received June 25, 1976; revision received Sept. 3, 1976. Work performed under NASA Prime Contract No. NAS 1-9000 and Martin Marietta Contract No. GC 1-095012.

References

[1]Huxtable, D., Marshall, G., Reck, M., and Hagemann, D., "Ground Simulation Testing of Hydrazine Monopropellant Gas Generators for Space Shuttle Auxiliary Power Unit," AIAA Paper 75-1272, Anaheim, Calif., 1975.

[2]Boltz, C. W., "Rocket Research Corporation Thermal Analyzer Program," RRC 68-ES-57 R1, 1969.

[3]Oppenheim, A. K., "Radiation Analysis by the Network Method," *ASME Journal*, May 1956, pp. 725–735.

[4]Schultz, H. D., "Thermal Analyzer Program for the Solution of General Heat Transfer Problems," Lockheed California Company, Sunnyvale, Calif., LR-18902, 1965.

[5]"Boeing Thermal Analyzer Engineering Usage Guide," The Boeing Company, Seattle, Wash., AS0315, 1962.

[6]Cunningham, C. R., "Viking Lander Capsule Rocket Engine Assembly Thermal Analysis Report," Rocket Research Corporation, Redmond, Wash., 71-R-273, revision B, Jan 1973, pp. 82–83, 86–93.

[7]Daly, J. M., "Viking Lander Capsule Rocket Engine Assmebly Stress and Dynamics Report," Rocket Research Corporation, Redmond, Wash., 72-R-290, Part I, revision B, Feb. 1973, p. 5-1.

[8]Kreith, F., *Principles of Heat Transfer*, 3rd ed., Intext Educational Publishers, New York, 1976, p. ix.